Ocean mesoscale eddies and vertical motion

Ananda Pascual[1]*, Peter Gaube[2^], Evan Mason[1], Bàrbara Barceló-Llull[3], Simón Ruiz[1]

(1) IMEDEA(CSIC-UIB), Mallorca, Spain
(2) Applied Physics Laboratory at the University of Washington, Seattle, US
(3) Universidad de Las Palmas de Gran Canaria, Gran Canaria, Spain
*Corresponding author: ananda@imedea.uib-csic.es, ^Presenting author: pgaube@apl.washington.edu

2016 OCEAN SCIENCES MEETING

Abstract

Oceanic mesoscale eddies are energetic features where strong three-dimensional circulations are set up and consequently enhanced biological activity take place. Indeed, vertical circulation associated with mesoscale eddies is of great importance as it may explain the patchiness of chlorophyll in the surface layers of the ocean. This work is focused on the estimation and analysis of the vertical exchanges associated with mesoscale dynamics and of their interannual variability, concentrating on selected areas of the World Ocean. We compute vertical velocities by integrating the quasi-geostrophic omega equation from an observational approach i.e., using the 3D fields of temperature and salinity derived from the ARMOR3D reanalysis that combines satellite (SST and altimetry) and in-situ (Argo profiling floats, XBT, CTD and moorings) data. The variability of the vertical velocity field is analyzed and the potential links between the observed signals and surface chlorophyll using tools for eddy identification and tracking are also investigated.

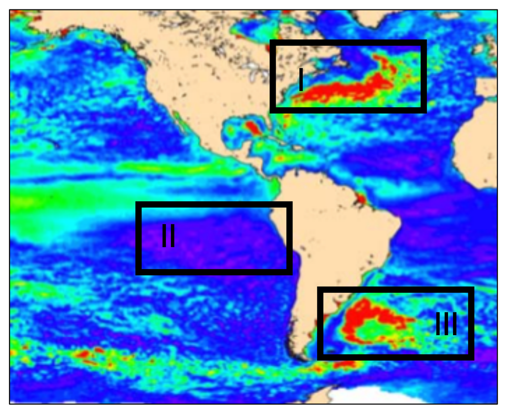

Fig. 1: The three zones analyzed in this work: Gulf Stream (I), South-East Pacific (II) and Brazil Malvinas-Confluence Region (III). The background map corresponds to rms of sea level anomaly variability from Pascual et al. (2006).

Vertical motion – Quasi-Geostrophic (QG) framework

$$\nabla_h^2\left(N^2 w\right)+f^2\frac{\partial^2 w}{\partial z^2}=2\nabla_h\cdot\vec{Q} \qquad \text{(Eq. 1)}$$

$$\vec{Q}=\left[f\left(\frac{\partial V}{\partial x}\frac{\partial U}{\partial z}+\frac{\partial V}{\partial y}\frac{\partial V}{\partial z}\right),-f\left(\frac{\partial U}{\partial x}\frac{\partial U}{\partial z}+\frac{\partial U}{\partial y}\frac{\partial V}{\partial z}\right)\right] \qquad \text{(Eq. 2)}$$

(U,V): geostrophic velocity components
w: quasi-geostrophic vertical velocity (QG-w)
Q: Q vector
N: Brunt-Vaisala frequency
f: Coriolis parameter

QG approximation valid for Ro = U/(f L) << 1

Ro: Rossby number
L: characteristic scale

Hoskins et al. (1978)
Tintoré et al. (1991)
Ruiz et al. (2009)

QG-w derived from synthetic fields

3D fields of temperature, salinity and steric height derived from an observational-based product that combines satellite (SST and altimetry) and in-situ (Argo profiling floats, XBT, CTD and moorings) data. (Guinehut et al. 2012).

Period: 1993-2009
Monthly fields
Domain: NW Atlantic

Zone I: Gulf Stream

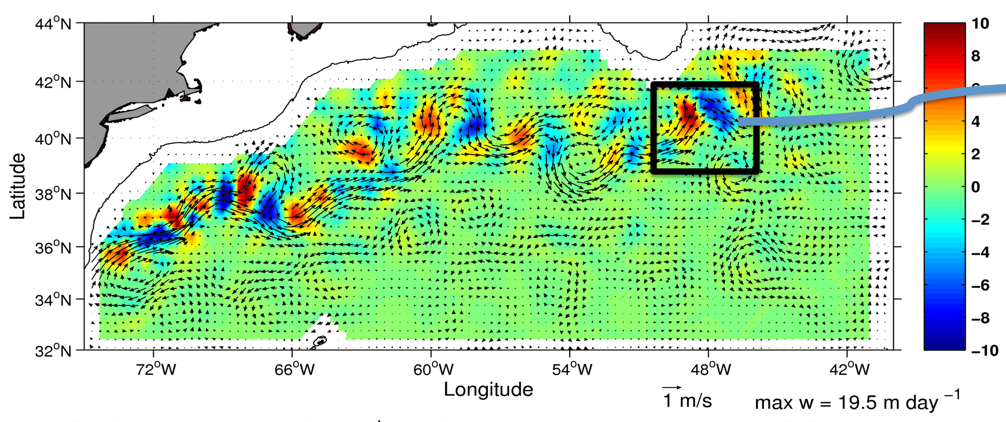

Fig. 2: Vertical velocity (m day^{-1}) at 100 m, obtained by integrating the QG omega equation from the 3D field of ARMOR3D corresponding to September 2005. Horizontal geostrophic currents are overimposed.

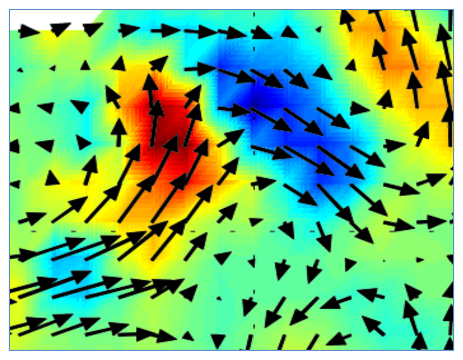

Upwelling (downwelling) upstream (downstream) of a meander crest. QG-w patterns are consistent with those predicted by QG theory (Pascual et al. 2004; Gomis et al. 2005)

How realistic are QG-w estimates compared to total w?

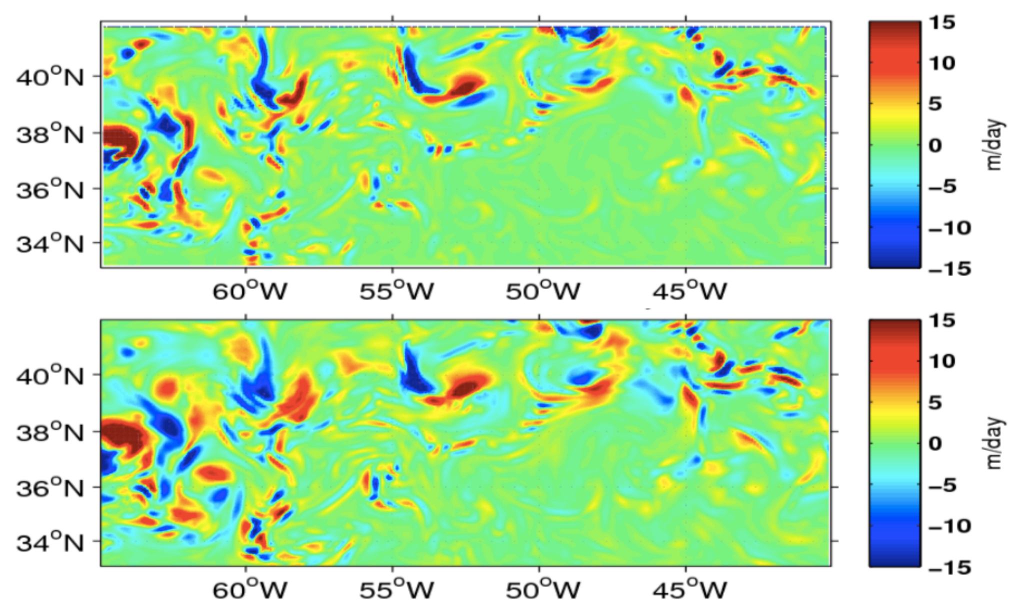

QG-w explains more than 70% of the model-w variance.

Fig. 3: Snapshot of QG-w (top) at 104 m estimated from temperature and salinity POP model fields (Anderson et al. 2011) and given POP vertical velocity (bottom). Correlation: 0.74.

NPP response to QG-w

Observed Net Primary Production (NPP)

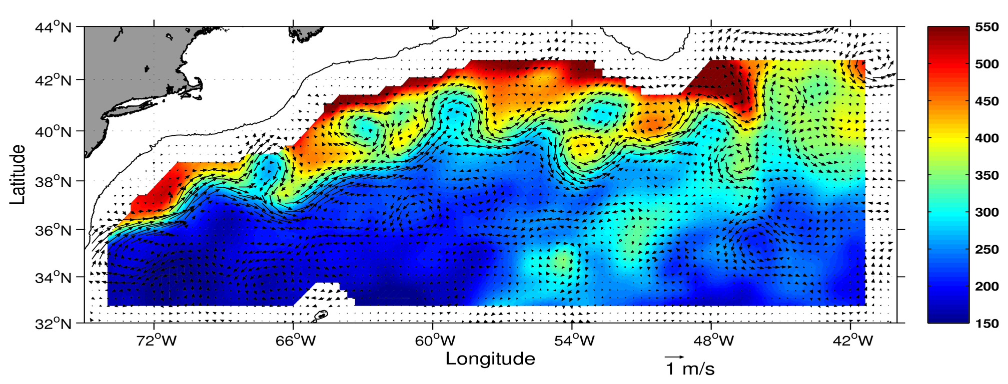

Fig.4: Horizontal geostrophic currents at 100 m derived from ARMOR3D data for September 2005. The colormap corresponds to the monthly mean of net primary production (mg C m-2 day-1) for the same month from Oregon State University.

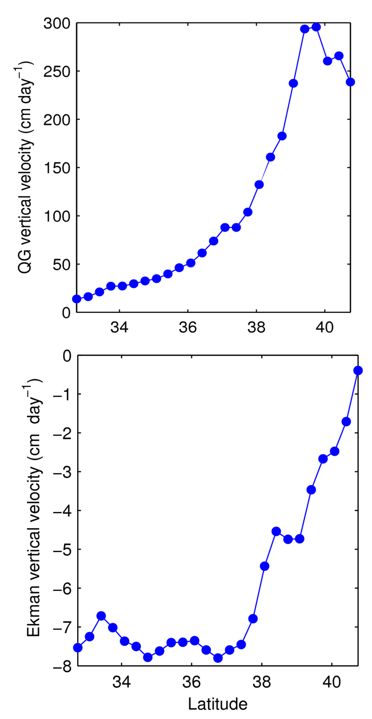

Fig. 5: Vertical velocity inputs for the application of the L11 model, as a function of latitude, averaged from 65°W to 40°W and over 1998-2009 period: (Top) Rms of QG-w at 100 m (cm day^{-1}); (Bottom) Climatological Ekman vertical velocity (cm day^{-1}).

Conceptual model by LATHUILIERE et al. 2011 (L11)

$$\mathrm{NPP}=\mu NP-mP=\frac{N}{H}\frac{\alpha^2+\alpha w_{Ek}}{\alpha+w_c-w_{Ek}} \qquad \text{(Eq. 3)}$$

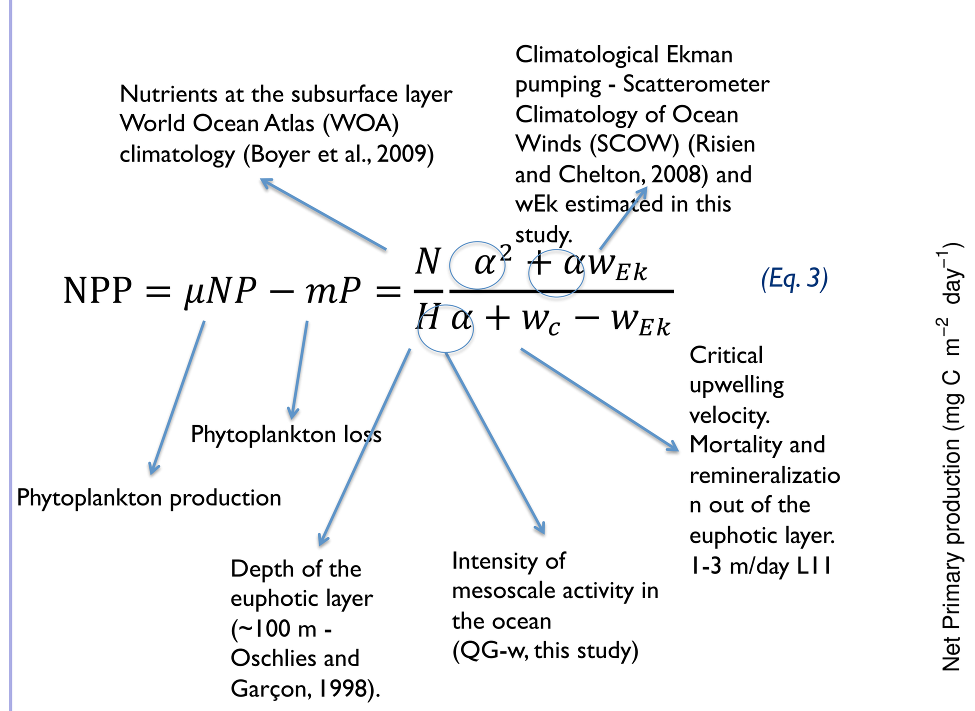

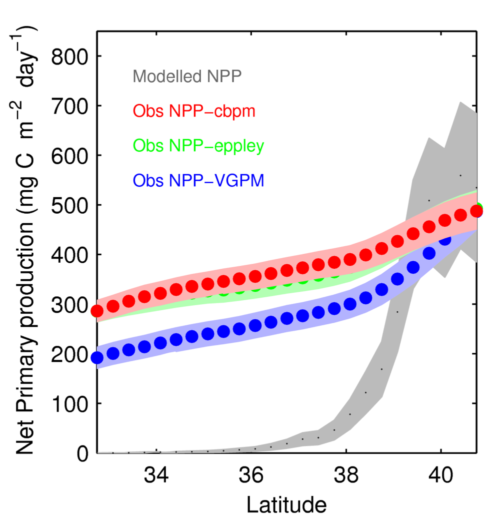

Fig. 6: Observed mean NPP (in blue the NPP-VGPM, green Eppley and red cbpm) versus modelled mean NPP (grey) as a function of latitude.

- More details in: Pascual et al. (2015)

Zone II: South-Eastern Pacific

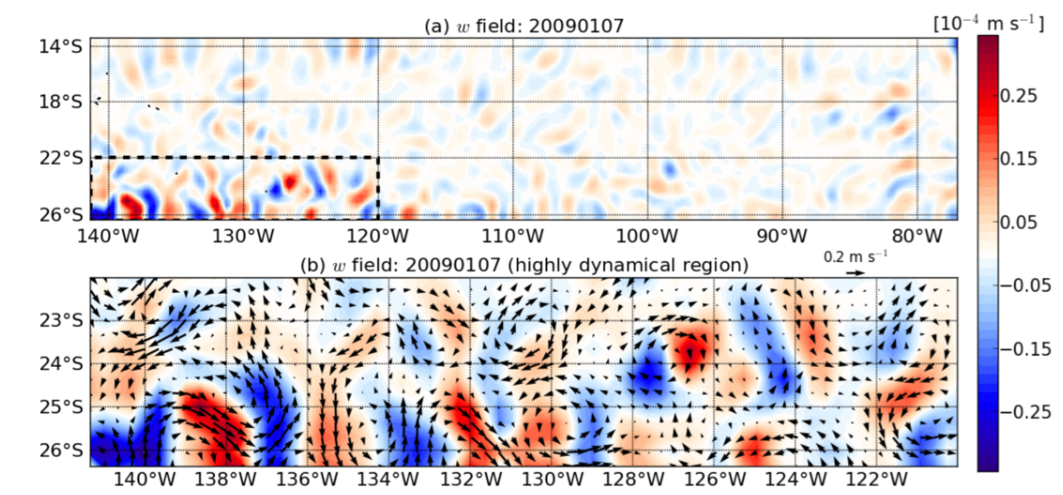

Fig. 7: (a) Vertical velocity on 7 January 2009 at 200 m depth. Black box delimits the region of high mesoscale eddy activity. (b) Zoom of vertical velocity and horizontal geostrophic currents over the high mesoscale eddy activity region in (a).

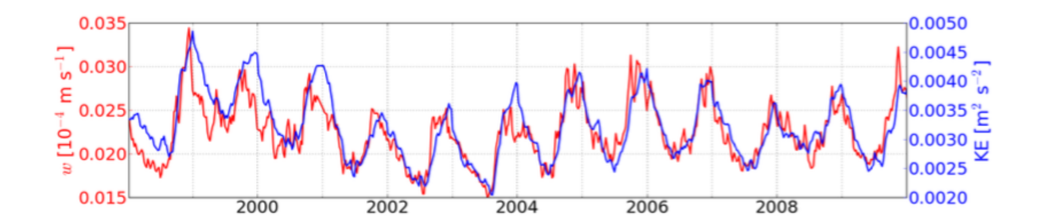

Fig. 8: Time series of vertical velocity magnitude (red line) and kinetic energy (blue line) averaged over the area of study. The correlation coefficient between vertical velocity and kinetic energy is 0.84.

An innovative approach is used to analyze the impact of vertical velocities associated with (QG) dynamics on the distribution of a passive nutrient tracer (nitrate) in the South East Pacific. Seasonal variability of QG vertical velocity and kinetic energy associated with the horizontal currents are coincident, with peaks in austral summer (November–December) in accord with published observations. Two ensembles of Lagrangian particle tracking experiments that differ according to vertical forcing (w = QG-w vs. w = 0) enable a quantitative analysis of the impact of the vertical velocity. From identical initial distributions of nitrate-tagged particles, the Lagrangian results show that the vertical velocities are responsible for creating nitrate changes whose level after 30 days is 30% of that created by horizontal advection alone. Despite being weaker by a factor of up to 10^{-4} than the horizontal currents, vertical velocity is demonstrated to make an important contribution to nutrient distributions in the region of study.

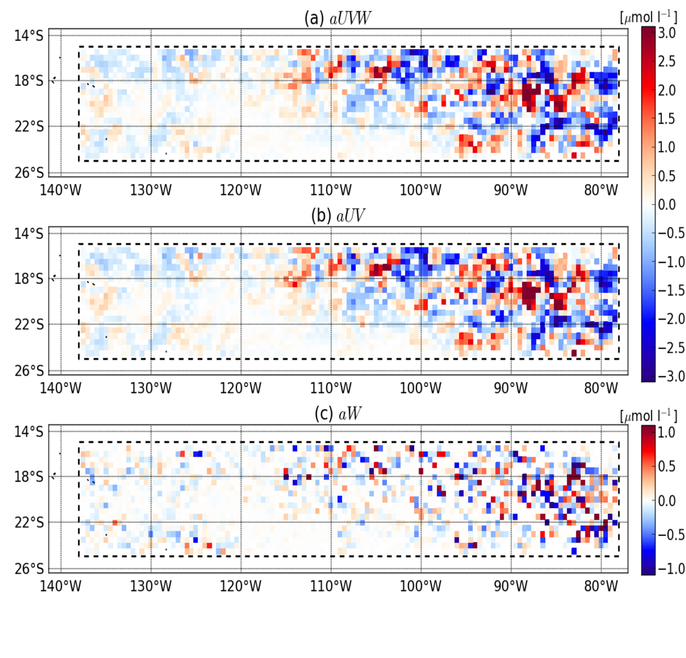

Fig. 9: Nitrate anomalies resulting from (a) contributions from both QG vertical velocity and geostrophic horizontal velocity (aUVW); (b) the contribution from only geostrophic horizontal velocity (aUV); and (c) the QG vertical velocity contribution (aW).

More details in: Barceló-Llull et al. (2015)

Zone III: Brazil-Malvinas Confluence Region

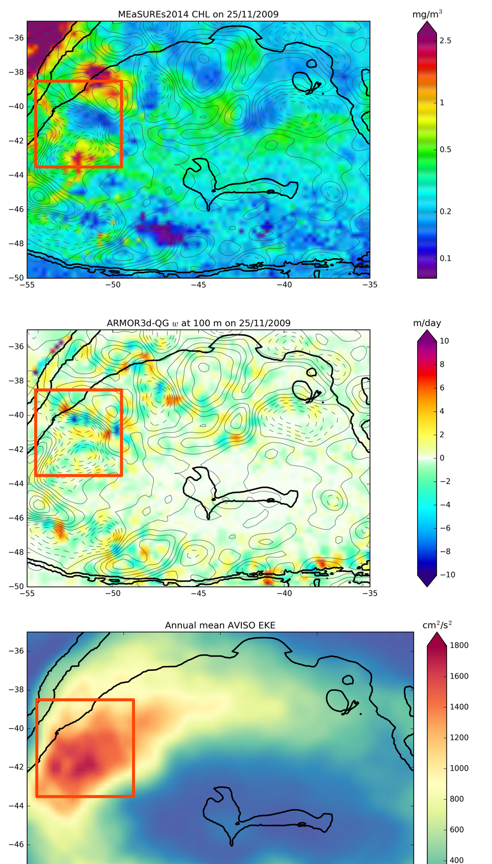

Fig 10: Snapshots over the Brazil-Malvinas Confluence region of (top) high-pass filtered daily CHL'' (from OB.DAAC and MEaSUREs2014 programs) and (middle) ARMOR3d weekly QG-w at 100 m depth on 25 November 2009. Both figures include the corresponding sea level anomaly from AVISO (thin grey contours; solid/dashed for anticyclones/ cyclones), and isobaths at 1000, 3000 and 5000 m depth. The red square corresponds to the area of maximum mean averaged EKE (see bottom pannel).

Eddy track coordinates and associated properties for the Brazil-Malvinas Confluence (BMC) region were obtained using the py-eddy-tracker code (Mason et al., 2014). The eddy-compositing approach is similar to that of Gaube et al. (2014). Here we take advantage of the daily observations to make composites of CHL' and QG-w (see Fig. 11 for cyclones). CHL'' takes the form of a strong positive monopole also reported by Gaube et al. (2014); the distribution is slightly asymmetric with maxima to the northeast of the mean eddy center. QG-w has a dipole distribution, with positive (negative) values located near the eddy periphery to the northwest (southeast); maxima are O(1 m day^{-1}). The QG-w north-south distribution can be understood in terms of conservation of potential vorticity (e.g., Villas-Boas et al., 2015). Further, the QG-w dipole could explain the asymmetry in CHL''. Since the flow is 3D, upwelled particles (nutrients for example) within the eddy also experience horizontal (top), which is located downstream (in the sense of the eddy coordinates) of the maximum QG-w upwelling at 100 m depth (Fig. 11b). The chlorophyll increase may reflect a direct response to the nutrients made available by the eddy dynamics.

The distributions and intensities of eddy-composite CHL'' and QG-w are seen to vary considerably across the BMC (not shown). In ongoing work we will address this variability and its sources (which may include the steep topography and the large-scale density fronts that characterize this energetic region).

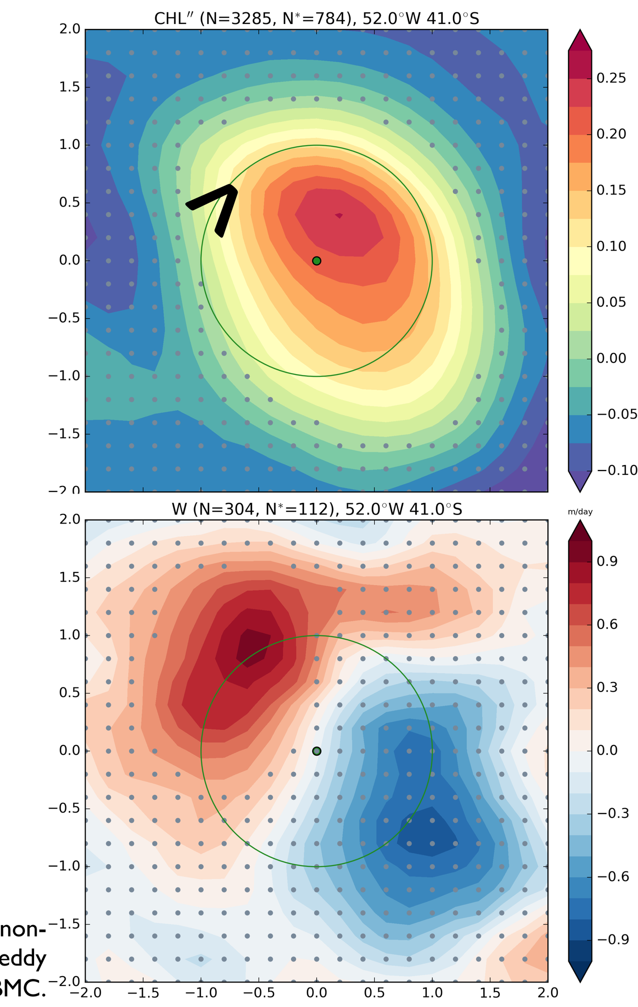

Fig 11: Eddy-centric composite averages of CHL'' (top) and QG-w (bottom) for cyclonic eddies. Dotted areas denote non-significant values at the 95% confidence level. Averages for anticyclones are non significant. The composites are made from eddy observations within the box outlined in red in Fig. 10, which corresponds to the region of maximum EKE in the BMC.

Acknowledgements

This work has been carried out in the frame of E-MOTION project (CTM2012-31014) funded by the Spanish National Research Program. EM is supported by a post-doctoral grant from the Conselleria d'Educació, Cultura i Universitats del Govern de les Illes Balears (Mallorca, Spain) and the European Social Fund.

REFERENCES

Anderson, L., D. McGillicuddy, M. Maltrud, I. Lima, and S. Doney (2011), Impact of eddy-wind interaction on eddy demographics and phytoplankton community structure in a model of the North Atlantic Ocean, Dyn. Atmos. Oceans, 52, 80–94.
Barceló-Llull, B.; E. Mason, A. Pascual. Impact of vertical and horizontal advection on nutrient distribution in the south east pacific. Ocean Science Discussion, 12, 2257-2281. 2015. doi:10.5194/osd-12-2257-2015, Under review for Ocean Science.
Capet, A.; E. Mason, V. Rossi, Ch. Troupin, Y. Faugère, I. Pujol, A. Pascual. Implications of Refined Altimetry on the Estimates of Mesoscale Activity and Eddy-Driven Offshore Transport in the Eastern Boundary Upwelling Systems. Geophysical Research Letters, 41-21, p 7602-7610. DOI: 10.1002/2014GL061770. October 2014.
Gaube, P., D. B. Chelton, P. G. Strutton, and M. J. Behrenfeld (2013), Satellite observations of chlorophyll, phytoplankton biomass, and Ekman pumping in nonlinear mesoscale eddies, J. Geophys. Res. Oceans, 118, doi:10.1002/2013JC009027.
Gaube, P., D. J. McGillicuddy Jr., D. B. Chelton, M. J. Behrenfeld, and P. G. Strutton (2014), Regional variations in the influence of mesoscale eddies on near-surface chlorophyll, J. Geophys. Res. Oceans, 119, doi:10.1002/2014JC010111.
Gomis, D., Pascual, A., and Pedder, M. A.: Errors in dynamical fields inferred from oceanographic cruise data: Part II. The impact of the lack of synopticity, Journal of Marine Systems, 56, 334-351, 2005.
Guinehut, S., Dhomps, A. L., Larnicol, G., and Le Traon, P.Y.: High resolution 3-D temperature and salinity fields derived from in situ and satellite observations, Ocean Science, 8, 845-857, 2012.
Lathuiliere, C., M. Levy, and V. Echevin, 2011: Impact of eddy-driven vertical fluxes on phytoplankton abundance in the euphotic layer. J. Plankton Res., 33, 827–831, doi:10.1093/plankt/fbq131.
Hoskins, B. J., I. Draghici, and H. C. Davies (1978), A new look at the omega-equation, Q. J. R. Meteorol. Soc., 104, 31–38.
Mason, E.; A. Pascual; J.C. McWilliams. A new sea surface height-based code for oceanic mesoscale eddy tracking. Journal of Atmospheric and Oceanic Technology. 31 - 5, pp. 1181 - 1188. 2014.
Pascual, A., D. Gomis, R. L. Haney, and S. Ruiz (2004), A quasigeostrophic analysis of a meander in the Palamos Canyon: Vertical velocity, geopotential tendency, and a relocation technique, Journal of Physical Oceanography, 34(10), 2274-2287.
Pascual, A., S. Ruiz, B. Buongiorno Nardelli, S. Guinehut, D. Iudicone, and J. Tintoré (2015), Net primary production in the Gulf Stream sustained by quasi-geostrophic vertical exchanges, Geophys. Res. Lett., 42, doi:10.1002/2014GL062569.
Ruiz, S., A. Pascual, B. Garau, I. Pujol, and J. Tintoré (2009), Vertical motion in the upper ocean from glider and altimetry data, Geophysical Research Letters, 36(14).
Tintoré, J., D. Gomis, S. Alonso, and G. Parrilla (1991), Mesoscale dynamics and vertical motion in the Alboran Sea, J. Phys. Oceanogr., 21, 811–823.
Villas Bôas, A. B., O. T. Sato, A. Chaigneau, and G. P. Castelão (2015), The signature of mesoscale eddies on the air-sea turbulent heat fluxes in the South Atlantic Ocean, Geophys. Res. Lett., 42, 1856–1862, doi:10.1002/2015GL063105.

Key Points

- New estimation of vertical velocity derived from an observational-based approach that combines in situ and satellite (altimetry and SST) data.
- QG-vertical velocities can sustain net primary production in the Gulf Stream.
- Lagrangian results in the South Eastern Pacific show that vertical velocities are responsible for nitrate redistribution with a signal variance of 1/3 of the associated with horizontal advection alone.
- Eddy-centric composite averages of CHL and QG-w in the Brazil Malvinas Currents, present some asymmetries that may reveal links between both variables.